buildings

MDPI

Article

Microscopic Mechanism and Reagent Activation of Waste Glass Powder for Solidifying Soil

Yuze Hong [1,2], Xinyi Xu [3,4], Chaojie Zhang [2,4,*], Zehai Cheng [1,*] and Guanshe Yang [5]

[1] Institute of Civil and Architectural Engineering, Zhejiang University of Science and Technology, Hangzhou 310023, China; hongyuze2021@163.com
[2] Zhejiang Provincial Key Laboratory of Water Conservancy Disaster Prevention and Mitigation, Hangzhou 310020, China
[3] Houston International Institute, Dalian Maritime University, Dalian 116026, China; xinyi_xu2003@163.com
[4] Zhejiang Institute of Hydraulics & Estuary, Hangzhou 310020, China
[5] Ningbo Raw Water Co., Ltd., Ningbo 315000, China; bgs.bx@163.com
* Correspondence: zcjie2004@126.com (C.Z.); chengzh2008@163.com (Z.C.)

Abstract: Glass waste products represent a significant environmental concern, with an estimated 1.4 billion tons being landfilled globally and 200 million tons annually. This results in a significant use of land resources. Therefore, it would be highly advantageous to develop a new method for disposing of waste glass. Waste glass can be recycled and ground into waste glass powder (WGP) for use in solidified soil applications as a sustainable resource. This study is based on solidified soil research, wherein NaOH, $Ca(OH)_2$, and Na_2SO_4 were incorporated as activators to enhance the reactivity of WGP. The optimal solidified soil group was determined based on unconfined compressive strength tests, which involved varying the activator concentrations and WGP content in combination with cement. X-ray diffraction (XRD) was used to study the composition of solidified soil samples. Microscopic pore characteristics were investigated using scanning electron microscopy (SEM), and the Image J software was employed to quantify the number and size of pores. Fourier-transform infrared spectroscopy (FTIR) was employed to examine the activation effect of waste glass powder. This study investigated the solidification mechanism and porosity changes. The results demonstrate that the addition of activated WGP to solidified soil enhances its strength, with a notable 12% increase in strength achieved using a 6% $Ca(OH)_2$ solution. The use of 2% concentration of Na_2SO_4 and NaOH also shows an increase in strength of 7.6% and 8.6%, respectively, compared to the sample without WGP. The XRD and SEM analyses indicate that activated WGP enhances the content of hydrates, reduces porosity, and fosters the formation of a more densely packed solidified soil structure.

Keywords: activation; solidified soil; strength; pore pattern; material content; Fourier-transform infrared spectroscopy

Citation: Hong, Y.; Xu, X.; Zhang, C.; Cheng, Z.; Yang, G. Microscopic Mechanism and Reagent Activation of Waste Glass Powder for Solidifying Soil. *Buildings* **2024**, *14*, 1443. https://doi.org/10.3390/buildings14051443

Academic Editor: Zengfeng Zhao

Received: 11 March 2024
Revised: 4 May 2024
Accepted: 9 May 2024
Published: 16 May 2024

1. Introduction

Waste glass can be effectively reused by converting it into waste glass powder (WGP) and incorporating it into solidified soil. Previous studies have explored the feasibility of reusing WGP [1,2]. However, the utilization of WGP poses several challenges despite its potential benefits. Firstly, glass and other utensils are typically found in a stable SiO_4 state, which complicates the transformation process from broken glassware to activated WGP. Furthermore, while WGP obtained through various processes contains essential hydroxide elements such as silicon and aluminum, it lacks calcium, which impedes its ability to achieve cohesive properties independently. Experiments have shown that substituting cement with inactivated WGP can reduce sample strength [3–5]. The successful resolution of the aforementioned challenges makes the potential of manufactured WGP immensely

significant. Many scholars have focused on glass powder as an auxiliary cement component. Gao X. [6] illustrated through in-depth thermal analysis that while the reactivity of WGP in a silicate cement system may be lower compared to fly ash, it shows remarkable similarity in an alkali-activated system, thereby substantiating the feasibility of using WGP as a substitute for fly ash. Additionally, it has been observed that WGP ground from glass of varying colors shows distinctive levels of reactivity [7–9]. In the area of particle dimensions, finely ground WGP possesses unique pozzolanic activity, Research has found [10–15] that glass contains a large amount of amorphous SiO_2, and there is also a high content of oxides such as Fe_2O_3 and Al_2O_3 in glass. As the particle size of glass powder decreases, it promotes the release of more amorphous SiO_2 and oxides, thus unveiling its promising potential as an adjunct cementitious component [16,17]. The particle size of WGP can be significantly diminished through the use of physical grinding techniques [18,19]. Studies have highlighted that WGP particles measuring below 100 μm are more adept at manifesting pozzolanic activity [20], particularly demonstrating the heightened reactivity of WGP particles beneath 38 μm [20–23]. Moreover, several academics posit [24] that the refinement of WGP plays a pivotal role in fortifying the strength of composite glass powder structures. This enhancement could be attributed to the meticulous dispersion of tiny WGP particles within the cement paste, ultimately contributing to a superior particle-size distribution of the cementitious material. Furthermore, the work of Yue Long [25] underscores the efficacy of alkaline activation in leaching WGP to generate active SiO_2. However, it is important to note that excessive alkali may incite alkali-aggregate reactions, which could reduce the strength and durability of the sample. Kong Qingqiu [26] conducted experiments which showed that WGP activated by a reagent has a significant early excitation effect and a later weakening effect. Conversely, Shi [27] believes that excitation of WGP by reagents can not only improve the early strength of the sample but also improve its later strength. In the area of microstructural examination, Li Zhuocai's electron microscopic investigations [28] unveiled a profusion of hydration byproducts that emerged during the latter phases of WGP specimens, crafting a compact, plate-like configuration. Meanwhile, the scholarly discourse exemplified by Zhang Chi et al. [29] postulates that the incorporation of WGP can diminish the macropores within a specimen. Conversely, Yu Xuanliang [30] suggests that WGP exhibits minimal impact on the quantity of macropores and capillary pores in a sample, but offers a moderate reduction in transition pore prevalence.

There are numerous applications of solidified soil, including roadbed backfilling, slope protection, and land reclamation. The incorporation of glass powder into this material could significantly enhance the global utilization rate of waste glass. Additionally, the selection of agents for solidifying soil is relatively extensive. This allows for the identification of the most suitable agent for a given engineering project based on factors such as strength and hazard classification. Therefore, in acid–base activation systems, reagent-activated WGP has great research potential in replacing silica fume, fly ash, and other materials. At present, there are many studies on the application of WGP in cement mortar or concrete, but there are few articles on the application of chemically activated WGP in cement-based solidified soil. This study focuses on the effect of activated WGP on the strength improvement of solidified soil, the changes in the microstructure of activated glass powder, the changes in sample composition, and the corrosive effect of reagents on waste glass powder.

This study activates glass powder through different concentrations of reagents and prepares solidified soil by mixing the activated WGP with cement according to different dosages. The mechanical properties of the soil are analyzed for its unconfined compressive strength. Additionally, the microstructure is characterized to evaluate changes in pore-size distribution through scanning electron microscopic (SEM) tests and the utilization of the Image J software for machine learning image processing. The composition of WGP-solidified soil and the alterations under different WGP activators are examined via X-ray diffraction (XRD) and Fourier-transform infrared spectroscopy (FTIR).

2. Experimental Section

2.1. Production of Glass Powder

This study explores the use of WGP as a coagulant additive, with cement as the main curing agent, by preparing solvent solutions with varying concentrations of 2%, 4%, and 6% using NaOH, $Ca(OH)_2$, and Na_2SO_4 as ingredients. The nuances of alkaline activation of OH^- ions versus sulfate ion activation, the solubility of Na ions, and the essential Ca^{2+} ion supplementation to counteract the natural calcium deficiency in WGP were explored, and a thorough evaluation of the activation effects and mechanisms was undertaken. In this experimental procedure, WGP was pre-activated, taking into consideration the weak acidic nature of the soil. Directly blending alkaline activators with WGP and introducing them to the soil may risk neutralizing the alkalinity. To prevent such disruptions and to enhance the interaction between the alkaline activator and WGP, as well as to promote the ease of pre-activating the WGP, the activation process unfolded as follows: (1) Opt for transparent and colorless glass vessels to ensure comparability during experimentation. (2) Employ ball milling for durations of 0 h, 6 h, and 12 h to produce distinct particle sizes of WGP. The particle-size distribution resulting from varying the ball milling durations is detailed in Table 1. (3) Immerse the utilized WGP from the 12 h ball milling process in 2%, 4%, and 6% concentrations of the reagent. (4) After a 3-day aging period in the solution, desiccate the WGP in a curing chamber at 40 °C until its moisture content is below 2%. (5) Following activation, reinstall the WGP in the ball mill for a final milling session, and sieve it through a 0.075 mm filter to yield the ultimate product for detecting the composition of glass, as shown in Table 2.

Table 1. Composition of WGP particle size at different milling times.

0 h	Particle-size composition			
Particle size (mm)	0.5–1	0.25–0.5	0.075–0.25	0–0.075
Content (%)	0.9	5.8	57.97	35.33
6 h	Particle-size composition			
Particle size (mm)			0.075–0.25	0–0.075
Content (%)			20.6	79.4
12 h	Particle-size composition			
Particle size (μm)	0–5.23	5.23–14.78	14.78–41.8	
Content (%)	29.16	28.37	42.47	

Table 2. Chemical composition of transparent bottle and jar glass.

SiO_2 (%)	Al_2O_3 (%)	CaO (%)	MgO (%)	Na_2O (%)	Fe_2O_3 (%)
72	2.5	8.25	2	14.6	0.1

2.2. Selection of Activators

The activator selection was evaluated based on two factors: the impact of the reagent itself on the hydration performance of cement and and the influence of the reagent on the WGP activity. The erosion effect of alkaline agents on WGP is closely related to the type of cation present, particularly Ca^{2+}. The solubility of the calcium salt formed on the glass surface is relatively low. However, in the presence of Na^+ as the cation, the resulting sodium salt can rapidly dissolve on the glass surface, hastening the erosion of the glass at greater depths [31]. Concurrently, the corrosive potential of OH^- ions is also notably strong. This highlights the noteworthy advantage of NaOH as an activator, with its corresponding reaction formula depicted as follows when SiO_2 is dissolving in an alkaline solution [32]:

$$\equiv\text{Si-O-Si}\equiv + \text{OH}- \rightarrow \equiv\text{Si-O}- + \text{HO-Si}\equiv \quad (1)$$

The reactions that can occur on the surface of WGP due to the presence of an alkaline solution are as follows:

$$Si(OH)_4 + NaOH \rightarrow [Si(OH)_3O]{-}Na^+ + H_2O \quad (2)$$

The properties of Na_2SO_4 render it an effective sulfate with activating qualities on WGP. When the partially reacted Na_2SO_4 is combined with the energized WGP in a cemented solidified soil system, $Ca(OH)_2$ produced post cement hydration interacts with Na_2SO_4, resulting in the formation of NaOH. This has further stimulating effect on cement and glass:

$$Na_2SO_4 + Ca(OH)_2 + 2H_2O \rightarrow CaSO_4 \cdot 2H_2O + 2NaOH \quad (3)$$

Simultaneously, the partially used Na_2SO_4 engages in a reaction with $Ca(OH)_2$ produced during cement hydration, releasing Ca^{2+} ions and initiating the formation of AFt. This process can be explained by the following chemical equation: Na_2SO_4 swiftly consumes the $Ca(OH)_2$ released during cement hydration, expediting the early stages of hydration:

$$AlO_{2\_} + Ca^{2+} + OH^- + {SO_4}^{2-} \rightarrow 3CaO \cdot Al_2O_3 \cdot CaSO_4 \cdot 32H_2O \quad (4)$$

Glass powder, akin to fly ash, lacks inherent strength when used alone or combined with NaOH stimulation [33]. Furthermore, $Ca(OH)_2$, acting as an activator, exerts a corrosive influence on the WGP itself. To give cementitious properties to mixtures containing WGP and fly ash, substances with lime-like properties must be added to the composite system to supplement the element of "calcium" in order to activate the reactivity of WGP and generate cementitious products similar to the hydration reaction of Portland cement. The presence of quicklime (CaO) or hydrated lime ($Ca(OH)_2$) is required.

2.3. Preparation

Different concentrations [8,26,34] (2%, 4%, and 6%) of solutions of different reagents (NaOH, $Ca(OH)_2$, and Na_2SO_4) were prepared to explore the optimal dosage of WGP after activation. Different concentrations and pH values result in different activation effects, and increasing the concentration of OH^- is beneficial for Si-O and Al-O. The unconfined compressive strength of WGP was analyzed to evaluate the effectiveness of different reagents in activating its reactivity. Microscopic analysis was conducted using X-ray diffraction (XRD), scanning electron microscopy (SEM), and Fourier-transform infrared spectroscopy (FTIR). Machine learning with the Image J software was used to process the electron microscopic images to study the mechanical properties and microscopic features of WGP within the cemented solidified soil system, and to investigate its curing mechanism and changes in porosity.

The concentration of the solidifying agent (cement) for the solidified soil was 20% (by mass percentage), with a certain moisture content. WGP was added to the solidified soil post activation in the form of an external additive. The designed dosage of WGP as an external additive was 1%, 3%, 5%, and 7% (calculated per individual specimen). Each group of WGP was activated with 2%, 4%, and 6% solvent concentrations, with 36 groups in total. To demonstrate the effect of activated WGP, non-activated WGP at 1%, 3%, 5%, and 7% was used as the control group. Three horizontal samples were taken from each group after curing for 14 days, and the average of the results was calculated (same as below); the unconfined compressive strength test results are shown in Figure 1.

According to Figure 1, with an increase in the dosage of non-activated WGP, the unconfined compressive strength shows a decreasing trend. A moderate amount of non-activated WGP has little impact on the strength of the specimens. Strength is controlled by cement, but when the dosage is excessive, a decreasing trend in strength is observed. Excessive WGP actually inhibits the hydration of cement, as also noted by Niyomukiza

JB [35] in their study, where a decrease in strength was observed for specimens after a WGP dosage of 7%.

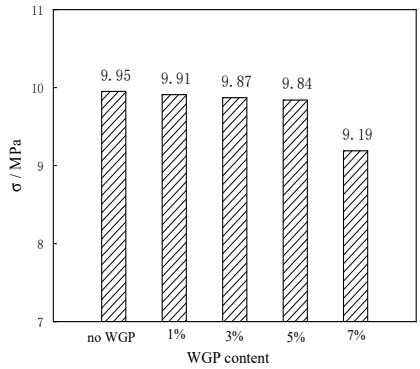

Figure 1. WGP content vs. unconfined compressive strength.

3. Results and Discussion

3.1. Unconfined Compressive Strength

Utilizing NaOH, $Ca(OH)_2$, and Na_2SO_4 as the reagents, the activators were prepared at concentrations of 2%, 4%, and 6% for glass activation. Post activation, WGP was blended at levels of 1%, 3%, 5%, and 7% into the samples, and the resultant powders were designated as NaOH waste glass powder (NWGP), $Ca(OH)_2$ waste glass powder (CWGP), and Na_2SO_4 waste glass powder (SWGP). Subsequent strength evaluation entailed the use of unconfined compressive strength testing. The strain rate of the experiment was 1 mm/min, and the maximum pressure of the sensor was 2000 kg. The unconfined pressure gauge and sensor are shown in Figure 2. Unconfined compressive strength is the most basic indicator for testing material properties in geotechnical tests. As it is not constrained by lateral forces, the results obtained can reflect the strength of the material. The WGP samples after testing are shown in Figure 3, and the results are shown in Figure 4.

Figure 2. Unconfined pressure instrument.

Figure 3. Damaged samples.

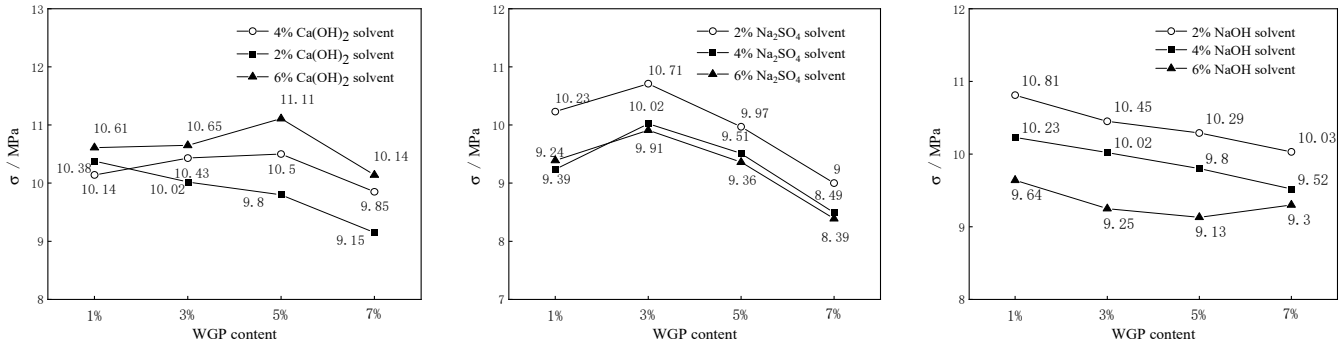

(**a**) (**b**) (**c**)

Figure 4. Curve of WGP content vs. strength. $Ca(OH)_2$ solvent (**a**), Na_2SO_4 solvent (**b**), NaOH solvent (**c**).

Based on the insights from Figure 4, it is evident that the WGP activated by a 6% concentration of $Ca(OH)_2$ solvent shows superior strength in comparison to powders activated by 2% and 4% concentrations. Furthermore, the WGP samples activated by 4% and 6% concentrations of $Ca(OH)_2$ exhibit an increase in strength with increasing dosage, with the 5% CWGP demonstrating the highest strength, suggesting that a 5% dosage is the most suitable. This finding aligns closely with the research by Wenwen Zhang [36]. Conversely, the strength of the WGP activated by 2% concentration $Ca(OH)_2$ tends to decrease as the dosage increases.

As shown in Figure 4b, the glass powder activated by 2% concentration of Na_2SO_4 solvent exhibits the most effective results. The SWGP samples produced by the three groups of solvents with different concentrations reflect a similar trend, showing an increase in strength as the SWGP dosage increases, with the highest unconfined compressive strength observed at a 3% SWGP. In Figure 4c, the activation effect of NWGP gradually diminishes with an increasing concentration of NaOH, resulting in a decrease in sample strength as the NWGP dosage increases.

These figures demonstrate that an inappropriate reagent dosage can weaken the WGP solidified soil after activation. Figure 4 shows that the unconfined compressive strength of each test group generally exceeds the corresponding control group's strength in Figure 1, indicating that utilizing the WGP activated by a 6% $Ca(OH)_2$ solvent has a noticeable effect on sample strength. Activation with $Ca(OH)_2$ serves to enhance the alkalinity of the samples and provides an ample supply of Ca^{2+} ions. This alkalinity is conducive to the pozzolanic activity of WGP, promoting the release of Al_2O_3, SiO_2, and other oxides. These oxides can interact with Ca^{2+} ions to generate hydration products like C-S-H and C-A-H, which are crucial for cement hardening. Therefore, the inclusion of WGP necessitates increased generation of $Ca(OH)_2$. Li Fang [24] conducted an experiment which showed a decrease in calcium and an increase in silicon and sodium content in the samples. This suggests that in the later stages of the experiment, the calcium element was consumed to produce hydration products like C-S-H, while $Ca(OH)_2$ separated the sodium and silicon elements from the WGP, further depleting the calcium content. Therefore, regardless of whether it is required to replenish the Ca^{2+} ion content or activate WGP, $Ca(OH)_2$ is a more suitable option. In terms of dosage, CWGP has an upper limit as excessive dosages increase the OH^- concentration in the solution, impacting the cement hydration process.

By analyzing the visual data depicted in Figure 4b, it is evident that at a 3% SWGP, each solvent concentration shows a peak unconfined compressive strength within its corresponding group. However, as the solvent concentration increases, the strength of the SWGP samples decreases. The addition of Na_2SO_4 accelerates the breakdown of the glass structure within the powder, thereby releasing more active SiO_2 and Al_2O_3, It also reacts chemically with $Ca(OH)_2$ decomposed from cement to generate C-S-H and C-A-H compounds (see Equations (5) and (6)). The generation of C-S-H and C-A-H compounds

results in a higher strength and increases the volume of hydration products, thus filling the pores of the sample and improving its strength. Yet, a high dosage of Na_2SO_4 (6%) triggers the formation of expansive ettringite, compromising the internal stability of the samples. Furthermore, the surplus ettringite stemming from an elevated Na_2SO_4 content depletes the levels of other hydration products. This conclusion is consistent with that of Xu Y.D. [37].

As shown in Figure 4c, it can be inferred that the critical threshold is reached at a 4% concentration of NaOH solvent. When the solvent concentration reaches 6%, the increased presence of OH^- ions in the solution interferes with the cement hydration process, resulting in a lower strength compared to the control group. During hydration, the concentration of Ca^{2+} is significantly affected by OH^-, whereby a higher liquid-phase OH^- content corresponds to a lower Ca^{2+} content. The decrease in Ca^{2+} concentration slows down the reaction rate and inhibits the formation of C-S-H and C-A-H compounds [38]. As noted in M. Ben Haha's study [39], it is observed that the potent activation of sodium hydroxide promptly engenders a C-S-H gel to envelope the WGP, impeding a substantial fraction of the powder from dispersing with free water to fill the larger pores, thereby contributing to the lowered strength. Similar reports have been conveyed by Ahmad S. Omran [40].

$$Ca(OH)_2 + A1_2O_3 + nH_2O \rightarrow CaO \cdot A1_2O_3\ (n + 1)\ H_2O \quad (5)$$

$$Ca(OH)_2 + SiO_2 + nH_2O \rightarrow CaO \cdot SiO_2 \cdot (n + 1)\ H_2O \quad (6)$$

3.2. Scanning Electron Microscopic (SEM) Analysis

Following a 14-day period of curing in a standard curing box, several representative groups of samples were selected from a large number of samples for this experiment. Each complete sample was dried in the shade and then cut into circular pieces with a diameter of 1 cm and a thickness of 0.5 mm, as shown in Figure 5. Attention was paid to break the observation surface of the sample to obtain a fresh cross-sectional opening. Finally, the sample was placed in a glass beaker, weighed, and dried in a vacuum drying oven. The vacuum pump was turned and the sample was dried in a vacuum environment at approximately 40 °C and 0.08 MPa for at least 24 h for later use. Before electron microscopic observation, it was necessary to fix the slices and apply a spray-gold treatment. The slices were adhered to the sample stage with conductive adhesive and a conductive film was sprayed on the surface of the slices, as shown in Figure 6. Once the spray coating process was finished, the sample was observed under an electron microscope. An electron microscopic image with a magnification of 10,000 X was selected to facilitate observation of the microstructure between the pores of the specimen.

Figure 5. Ring-cut specimen.

Figure 6. Samples on the loading platform.

Figure 7 shows a pure cement-based solidified soil sample, while Figures 8–10 show WGP solidified soil samples activated by NaOH, $Ca(OH)_2$, and Na_2SO_4, respectively. After pressure forming, the micrograph of the pristine cement-based solidified soil, depicted in Figure 7, in the cement control group displays an unconventional arrangement of particles. The surfaces of the soil particles are predominantly characterized by flake-like structures that spread out in a scattered manner, contributing to a loosely structured composition. The primary contact mode between particles was observed to be face-to-face. The sample, overall, shows a continuous, flattened clay mineral matrix, with visible localized accumulations of flat soil particles. After the original sample was magnified by 10,000 times, the flocculent hydration products of the thin film were observed to be stacked together in a face-to-face contact form. Locally, the oriented arrangement of the aggregates is visible, and a significant amount of C-S-H and AFt hydrates is distributed on the concave surface and pores. In contrast, following the introduction of WGP, the porosity of the sample surface notably decreases. The flake-like hydrated products exhibit an increase in surface area and thickness, become more uniform, and have greater integrity.

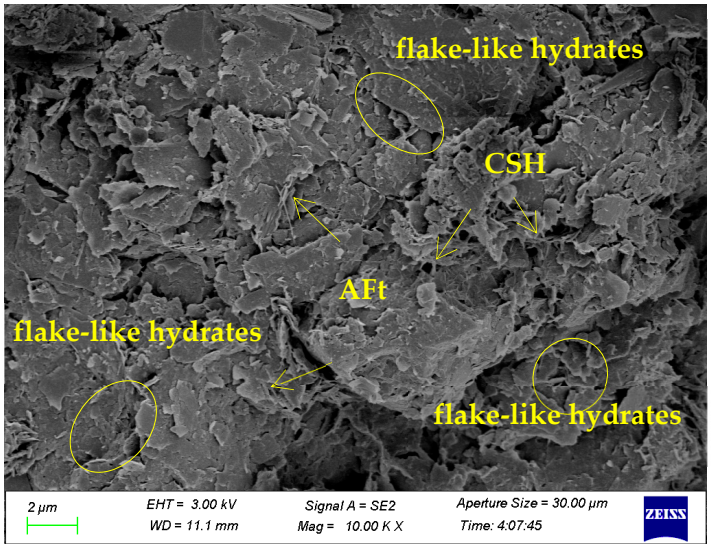

Figure 7. Cement-based solidified soil.

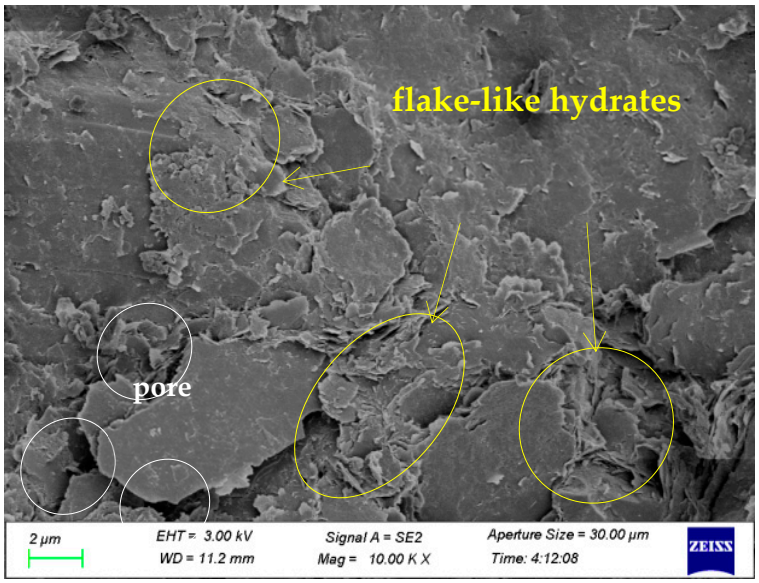

Figure 8. Solidified soil with CWGP.

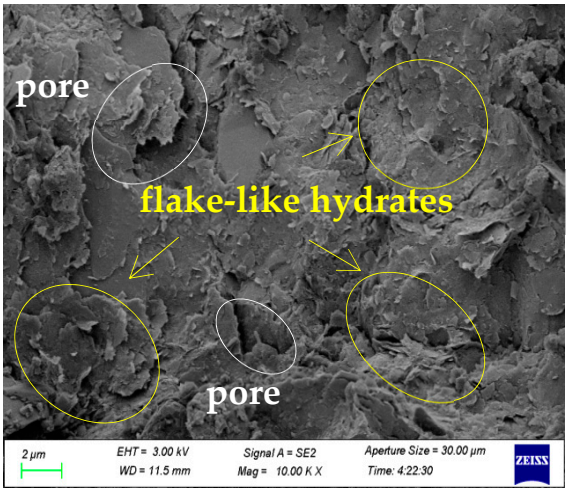

Figure 9. Solidified soil with SWGP.

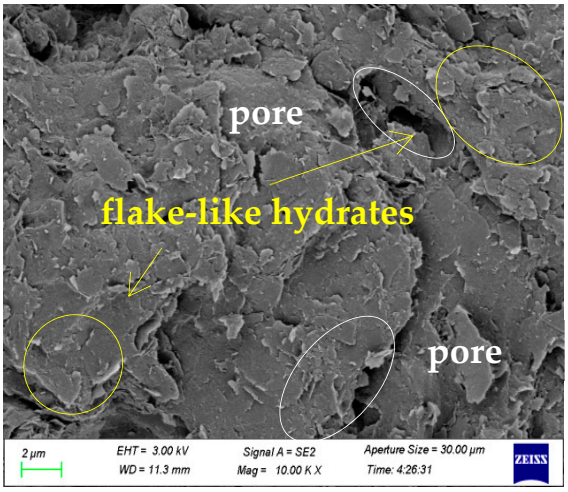

Figure 10. Solidified soil with NWGP.

From Figure 8, it can be observed that the sample surface is more compact, characterized by the distribution of thin flake-like hydrated products on top of plate-like solidified soil particles or within the interparticle voids. A comprehensive observation of the various hydrated flake-like products in the solidified soil reveals that the plate-like hydrated products in the group activated by $Ca(OH)_2$ and WGP exhibit larger areas and tighter integration. By observing Figures 9 and 10, it can be seen that despite having large plate-like hydration products, there are still pores between them. The key distinction between Figures 8–10 lies in the use of different activators for the WGP. The incorporation of $Ca(OH)_2$ leads to an increase in the area of hydrated products, enhancing uniformity and compactness. Based on the mechanical performance results in the previous section, the unconfined compressive strength of the WGP group activated by $Ca(OH)_2$ is the highest, corresponding to the denser hydration described in this section.

Figure 9 shows the NWGP group, which exhibits a small amount of flake-like hydrates. A large amount of the flat solidified soil mineral matrix is exposed to the outside. The flake-like hydrates do not attach as much to the surface of the solidified soil, as shown in Figures 7, 8 and 10. Some of them grow and are embedded between solidified soil particles, with a small amount attached to the surface. The hydration products attached to the solidified soil are relatively dense, with small pores, which also provides a certain strength for the sample. The distribution of flake-like hydration products in Figures 7 and 10 is similar, with the difference being that the flake-like hydration products in Figure 10 have a larger area. Compared with Figure 7, the larger flake-like hydration products cover or effectively fill the pores, providing a better overlap effect between soil particles. The surface of the sample is denser, which improves its mechanical properties.

3.3. ImageJ Microstructure Analysis

The image processing in this study employed a consistent electron microscopic magnification of 10,000 times. The software's advanced Intelligent processing capabilities were used for automated learning, a series of images underwent processing, pores were segmented, and different pore sizes were distinguished, culminating in the creation of Figures 11 and 12.

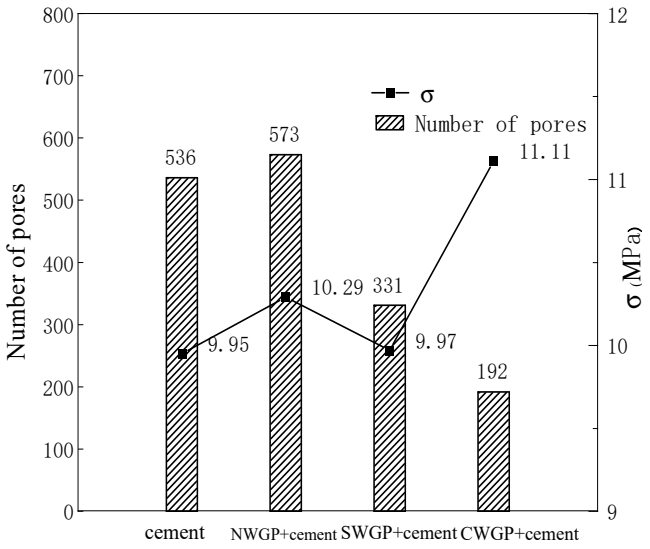

Figure 11. Diagram of the relationship between stress and pore quantity.

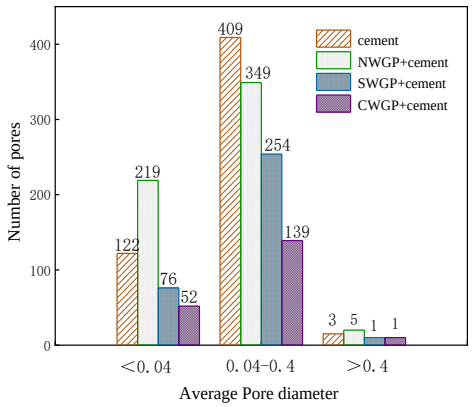

Figure 12. Pore sizes of glass powders with different activators.

The changes in pore quantities have a marginal impact on the samples' unconfined compressive strength, as demonstrated by the results shown in Figure 11, where a marked reduction in pores is evident in the CWGP samples, resulting in a significant increase in unconfined compressive strength compared to the other three groups. From Figure 12, it can be seen that the introduction of SGWP and CWGP led to a reduction in the range of pore sizes (pores less than 0.04 μm, pores between 0.04 μm and 0.4μm, and pores exceeding 0.4 μm) to varying degrees, The introduction of NWGP noticeably decreased the size of pores with a diameter of 0.04 μm to 0.4 μm to smaller dimensions (below 0.4 μm). In summary, the activated WGP can significantly improve the porosity of the samples compared to the pure cement experimental group, and the WGP activated by $Ca(OH)_2$ has the best porosity improvement effect.

Firstly, when analyzing for the main causes, compared with the experimental group without WGP, the medium porosity is significantly reduced and the waste glass powder particles are mostly angular in shape, which have the effect of filling the pores with micro-aggregates and are beneficial for improving the pore structure of the system and increasing density [41]. Secondly, the samples mixed with glass powder are prone to $Ca(OH)_2$ reaction, and a circle of hydrates forms around the glass powder, making the pores filled by the glass powder more dense [33]. In addition, excess $Ca(OH)_2$ is prone to $CaCO_3$ reaction when in contact with CO_2, as shown in reaction Formula (7). $CaCO_3$ is a sheet-like crystal attached to the surface of the sample, which is similar to the morphology shown in Figure 4, playing a role in reducing pores and increasing density. Moreover, it can be seen from reference [42] that the product of the reaction between SO_2 dissolved in WGP and $Ca(OH)_2$ is denser than the product of cement hydration.

$$Ca(OH)_2 + CO_2 \rightarrow CaCO_3 + H_2O \quad (7)$$

3.4. X-ray Diffractometer (XRD) Analysis

To further explore the influence of different activators on the composition of cement-based solidified soil samples, we used a multi-group trial and selected three representative groups from a large number of samples. In the early stage of the experiment, it was necessary to dry the samples using traditional shade drying and other drying methods. After shade drying, the samples were placed in a vacuum drying oven to ensure complete evaporation of moisture. After the samples were dried, they were ground into powder with a hammer and screened through a 0.074 mm sieve. About 10 g of each sample was prepared for testing.

Figure 13a–c show the X-ray diffraction patterns of the samples resulting from the introduction of WGP within the cemented solidified soil system. The patterns indicate that the chemical reactions began within 14 days. A detailed analysis uncovers that the mineral micro-components predominantly consist of kaolinite ($Al_2Si_2O_5(OH)_4$), silica (SiO_2), illite ($KAl_2[(SiAl)_4O_{10}]\cdot(OH)_2\cdot nH_2O$), albite ($Na(AlSi_3O_8)$), and the cementitious

material, hydrated calcium silicate (C-S-H). Each detected component displays distinct characteristic peaks on the diffraction profile. These components' relative proportions are visually represented in Figure 13a–c, which portray the primary constituents formed within the samples. From the detected components, it can be observed that the main components of WGP activated by different solvents did not change after being added to the solidified soil, but the proportion of its components changed slightly.

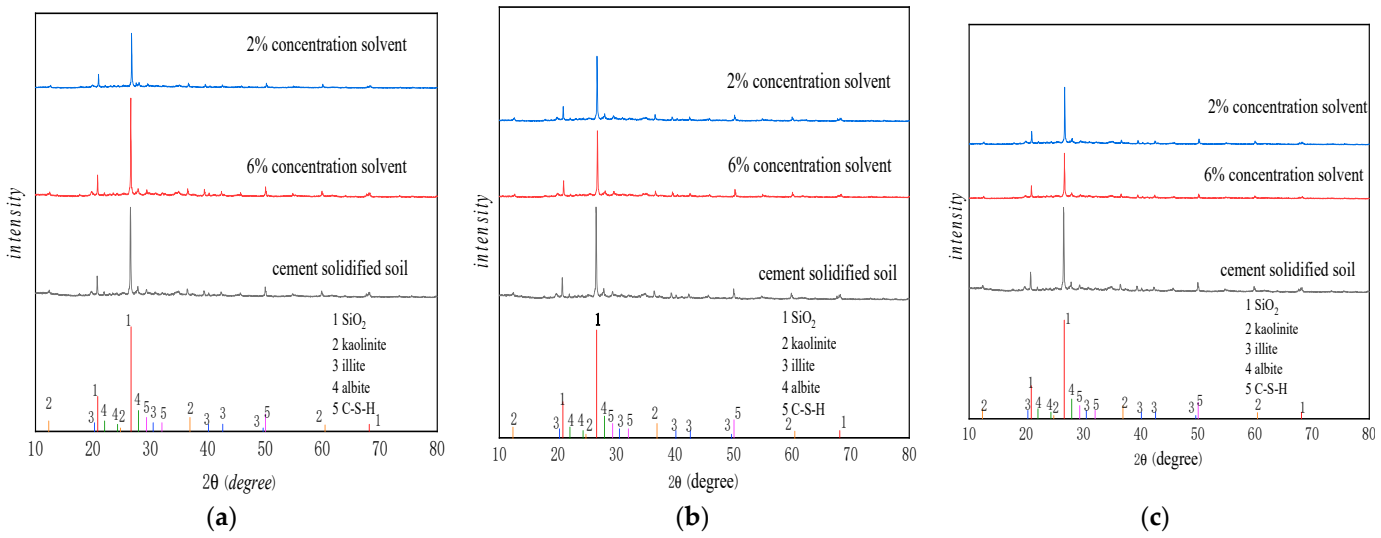

Figure 13. Different solvent concentrations of $Ca(OH)_2$ (**a**), Na_2SO_4 (**b**), and NaOH (**c**).

With the addition of glass powder, it can be seen that the SiO_2 content in Figure 14b and Figure 14c increases by 2% and 2.2%, respectively, compared to 30.9% in Figure 14a. The proportion of SiO_2 in Figure 14b is lower than that in Figure 14c, and the corresponding proportion of C-S-H gel in Figure 14b is higher. It can be seen that a certain amount of active SiO_2 has reacted to form C-S-H gel. This phenomenon is consistent with the above conclusion that the strength of WGP with 6% solvent is higher than that with 2% solvent. At the same time, the mineral composition of the original clay, such as kaolinite and illite sodium feldspar, shows slight changes in content due to the heterogeneity of the soil.

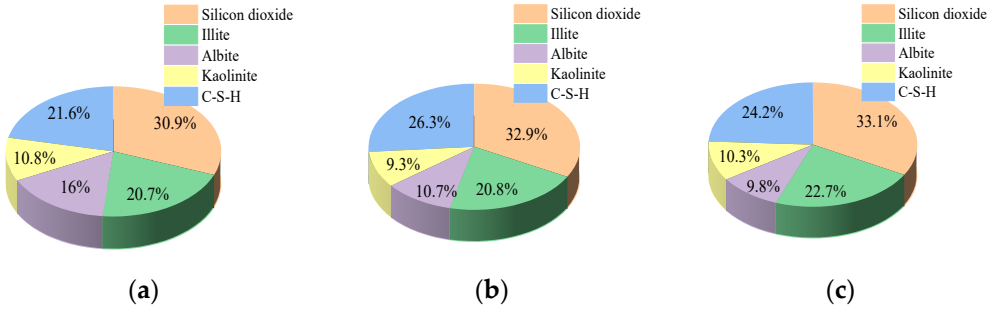

Figure 14. Mineral content ratio of $Ca(OH)_2$ WGP solidified soil. Solidified soil with (**a**) no glass powder; (**b**) 6% concentration solvent; and (**c**) 2% concentration solvent.

It is evident that the SiO_2 and C-S-H gel contents in Figure 15c surpass those in Figure 15b. The heightened presence of Na_2SO_4 causes a fracturing of the SiO_4 tetrahedra structure, rendering the reactive SiO_2 more vulnerable to hydration reactions. Consequently, there is a decline in SiO_2 content, as depicted in the compositional charts. In Figure 15b, the C-S-H gel content is lower than in Figure 15c, potentially attributed to the excessive consumption of $Ca(OH)_2$ by the increased Na_2SO_4 content during cement hydration. This leads to an overabundance of AFt, which depletes Ca^{2+} ions and impedes the formation of additional C-S-H gel, thereby contributing to the decrease in sample strength.

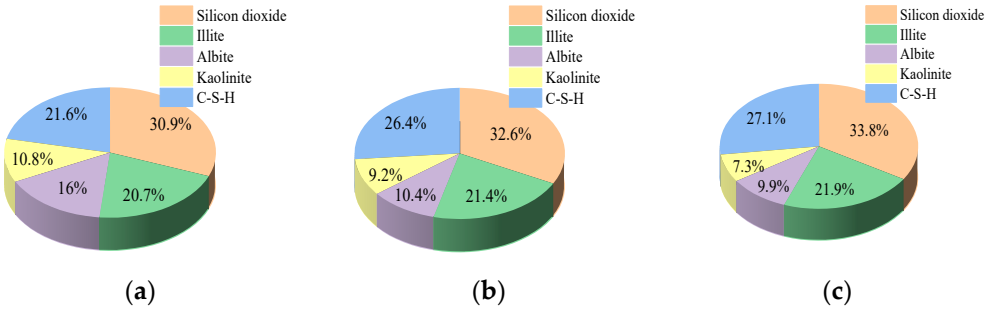

Figure 15. Mineral content ratio of Na_2SO_4 WGP solidified soil. Solidified soil with (**a**) no glass powder; (**b**) 6% concentration solvent; and (**c**) 2% concentration solvent.

Although sodium salts dissolve readily in water, an excess of NaOH increases the internal alkalinity of the sample, accelerating the reaction. Activated Al_2O_3 and SiO_2 in cement accelerate dissolution. The accelerated reactions promote the rapid formation of C-S-H gel surrounding the WGP, limiting the activation of most of the WGP; this explains the noticeable decrease in SiO_2 content in Figure 16c compared to Figure 16b. The increased active SiO_2 then participates in reactions that result in a greater abundance of C-S-H gel.

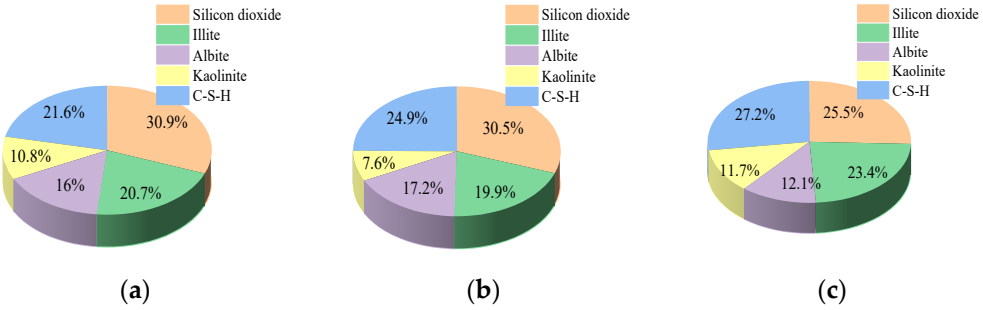

Figure 16. Mineral content ratio of NaOH WGP solidified soil. Solidified soil with (**a**) no glass powder; (**b**) 6% concentration solvent; and (**c**) 2% concentration solvent.

3.5. Fourier-Transform Infrared Spectroscopic (FTIR) Analysis

Based on the composition analysis of XRD described in the previous section, this study investigated the effect of activators on SiO_2 in WGP and further investigated the activation effect of NaOH, $Ca(OH)_2$, and Na_2SO_4 on WGP. Fourier-transform infrared (FTIR) spectroscopy was employed in the investigation. Inactive WGP and activators at 2% and 6% concentrations were chosen to enhance comparability. The experimental results are illustrated in Figures 17–19.

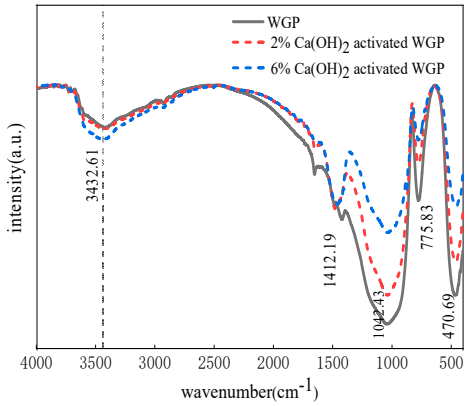

Figure 17. WGP activated by $Ca(OH)_2$ solvent.

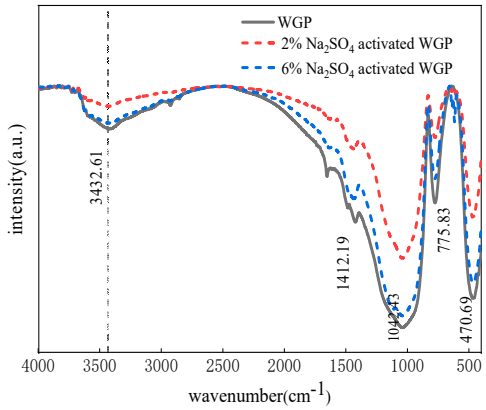

Figure 18. WGP activated by Na_2SO_4 solvent.

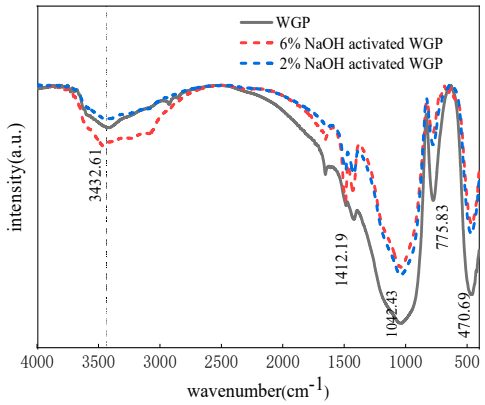

Figure 19. WGP activated by NaOH solvent.

In these figures, it is clear that the vibration peak position of the activated WGP closely matches that of the inactive WGP. However, there is a noticeable shift in the (Si-O-Si) bending vibration peak around 470.69 cm^{-1}, indicating the interaction of the activator with SiO_2 in the WGP. When comparing these three sets of graphs, it is evident that as the activator concentrations increase, the vibrational peak intensity decreases to varying degrees. This indicates the corrosive effect of activator concentration on SiO_2, causing chemical bonds to break.

The Si-O bond exhibits a symmetric stretching vibration peak at 775.83 cm^{-1}, while the Si-O-Si bond displays an antisymmetric stretching vibration peak at 1042.43 cm^{-1}. Both peaks vary proportionally with changes in the reagent concentration.

The distinctive peak residing near 1412.19 cm^{-1} arises from the presence of C-O bonds. This is likely due to carbonization effects during the meticulous sample preparation process, which might have led to the formation of carbonates within the sample [43–47]. Notably, the interaction of $Ca(OH)_2$ with CO_2 results in the production of $CaCO_3$, accentuating the peak broadening near 1412.19 cm^{-1} shown in Figure 17.

The intensification of the OH vibration peak at 3432.61cm^{-1}, displayed in both Figures 13 and 15, could be due to the nuanced alterations in vibration peaks induced by the introduction of NaOH and $Ca(OH)_2$. Conversely, in Figure 17, the peak's attenuation may be attributed to further consumption throughout the reaction process due to the absence of OH doping.

Moreover, an analysis of Figures 17 and 19 reveals that the vibration peaks of the $Ca(OH)_2$ solvents at 2% and 6% concentrations are significantly weaker compared to the 6% NaOH solvent, indicating the former has a greater ability to promote OH^- reactions, which may be due to a better activation effect. The vibration peak of NaOH solvent with a concentration of 2% is shallower than that of the original WGP, indicating the solvent

consumes both the original OH^- and itself. This further demonstrates that an appropriate concentration has a better activation effect, which is consistent with the previous results.

4. Conclusions

This study excited glass activity through different types of reagents and solvents at different concentrations. It used WGP of different dosages after activation to mix with cement-based solidified soil. The optimal dosage, optimal activator, and optimal concentration of the activator were obtained through unconfined compressive strength analysis. Scanning electron microscopic (SEM) experiments were performed and the Image J software for machine learning was used to process the electron microscopic images, characterizing their microstructure and analyzing the changes in pore size. Through X-ray diffraction (XRD) experiments, the composition of the glass powder solidified soil and the changes in composition content under different glass powder activators were analyzed, and the activation effect of waste glass powder was demonstrated through Fourier-transform infrared (FTIR) spectroscopy. The conclusions are as follows:

(1) The activation effect of different reagents on glass powder is influenced by their concentration. Unconfined compressive strength tests were conducted on samples of solidified soil mixed with glass powder to characterize their strength. The optimal concentration for the $Ca(OH)_2$ solvent is 6%, while the optimal concentration for the Na_2SO_4 and NaOH solvents is 2%.

(2) The comparative experiments revealed that the strength of the WGP solidified soil samples exhibited a gradual decline with the addition of glass powder. However, when glass powder was activated by the 6% $Ca(OH)_2$ solvent and was added at a dosage of 5%, the optimal dosage was obtained. The highest strength of the solidified soil produced was 11.11 MPa, which represented a 13% increase in strength compared to the inactive 5% dosage.

(3) Through SEM testing, it was found that the experimental group with added activated glass powder had a more uniform and denser microstructure compared to the pure cement experimental group. At the same time, compared with NWGP and SWGP groups, the pore size of the CWGP solidified soil group significantly reduced, and the large pore size tended to transform into a small pore size. The main reason is that CWGP can fill the pores and induce crystallization of $Ca(OH)_2$.

(4) The X-ray diffraction (XRD) analysis revealed that the predominant components of the solidified soil mixture with glass powder are kaolinite, silica, illite, albite, and cementitious material C-S-H. The addition of WGP is reflected in the pie chart by an increase in the content of SiO_2. With an appropriate solvent concentration, the C-S-H gel exhibits varying degrees of increase in the pie chart, thereby enhancing the strength of the solidified soil to a certain extent. This phenomenon reflects the activating effect of the activator and the feasibility of adding activated WGP to solidified soil.

(5) According to the Fourier-transform infrared (FTIR) spectroscopic analysis, as the reagent concentration increases, SiO_2 in the WGP continues to corrode the bond cleavage and the content of OH^- decreases accordingly.

Author Contributions: Conceptualization, Y.H., C.Z. and Z.C.; Methodology, Y.H., C.Z. and Z.C.; Software, Y.H. and X.X.; Validation, Y.H.; Formal analysis, Z.C.; Investigation, Y.H. and X.X.; Data curation, Y.H. and X.X.; Writing—original draft, Y.H.; Writing—review & editing, Y.H. and X.X.; Supervision, G.Y.; Project administration, Y.H. and G.Y.; Funding acquisition, G.Y. All authors have read and agreed to the published version of the manuscript.

Funding: This study was conducted by the Science and Technology Project of Zhejiang Provincial Depart- 312 ment of Water Resources, grant number RA1910; Science and Technology Project of Zhejiang Pro- 313 vincial Department of Water Resources, grant number RB2021.

Data Availability Statement: The original contributions presented in the study are included in the article, further inquiries can be directed to the corresponding authors.

Conflicts of Interest: Author Yang Guanshe was employed by the company Ningbo Raw Water Co., Ltd. The remaining authors declare that the research was conducted in the absence of any commercial or financial relationships that could be construed as a potential conflict of interest.

References

1. Jain, J.A.; Neithalath, N. Chloride transport in fly ash and glass powder modified concretes—Influence of test methods on microstructure. *Cem. Concr. Compos.* **2010**, *32*, 148–156. [CrossRef]
2. Nassar, R.U.D.; Soroushian, P. Green and durable mortar produced with milled waste glass. *Mag. Concr. Res.* **2012**, *64*, 605–615. [CrossRef]
3. Li, A.; Qiao, H.; Li, Q.; Hakuzweyezu, T.; Chen, B. Study on the performance of pervious concretemixed with waste glass powder. *Constr. Build. Mater.* **2021**, *300*, 123997. [CrossRef]
4. Khmiri, A.; Chaabouni, M.; Samet, B. Chemical behaviour of ground waste glass when usedas partial cement replacement in mortars. *Constr. Build. Mater.* **2013**, *44*, 74–80. [CrossRef]
5. Shayan, A.; Xu, A. Value-added utilisation of waste glass in concrete. *Cem. Concr. Res.* **2004**, *34*, 81–89. [CrossRef]
6. Gao, X.; Yu, Q.; Li, X.; Yuan, Y. Assessing the modification efficiency of waste glass powder in hydraulic construction materials. *Constr. Build. Mater.* **2020**, *263*, 120111. [CrossRef]
7. Song, B. Experimental Study on Activation of Waste Glass Powder. Master's Thesis, Nanhua University, Chiayi, China, 2013.
8. Du, H.J.; Tan, K.H. Use of waste glass as sand in mortar: Part II-alkali-silicareaction and mitigation methods. *Cem. Concr. Compos.* **2013**, *35*, 118–126. [CrossRef]
9. Zhao, H.; Ke, G.; Song, B.; Zou, P. Effect of waste glass pow der on hydration products of cement paste and structure of plastic sand. *Concrete* **2018**, *10*, 106–109+122.
10. Ali, E.E.; Al-Tersawy, S.H. Recycled glass as a partial replacement for fine aggregate in self compacting concrete. *Constr. Build. Mater.* **2012**, *35*, 785–791. [CrossRef]
11. Lam, C.S.; Poon, C.S.; Chan, D. Enhancing the performance of pre-cast concrete blocks incorporating waste glass e ASR consideration. *Cem. Concr. Compos.* **2007**, *29*, 616–625. [CrossRef]
12. De Moura, A.A.; Effting, L.; Moisés, M.P.; Carbajal, G.G.A.; Tarley, C.R.T.; Câmara, E.; Gracioli, A.; Bail, A. The influence of calcium-rich environments in siliceous industrial residues on the hydration reaction of cementitious mixtures. *J. Clean. Prod.* **2019**, *225*, 152–162. [CrossRef]
13. Geng, C.; Wu, X.; Yao, X.; Wang, C.; Mei, Z.; Jiang, T. Reusing waste glass powder to improve the strength stability of cement at HTHP. *J. Pet. Sci. Eng.* **2022**, *213*, 110394. [CrossRef]
14. Varma, D.N.; Singh, S.P. A Review on Waste Glass-based Geopolymer Composites as a Sustainable Binder. *Silicon* **2023**, *15*, 7685–7703. [CrossRef]
15. Cai, Y.; Xuan, D.; Poon, C.S. Effects of nano-SiO_2 and glass powder on mitigating alkali-silica reaction of cement glass mortars. *Constr. Build. Mater.* **2019**, *201*, 295–302. [CrossRef]
16. Schwarz, N.; Cam, H.; Neithalath, N. Influence of a fine glass powder on the durability characteristics of concrete and its comparison to fly ash. *Cem. Concr. Compos.* **2008**, *30*, 486–496. [CrossRef]
17. Yang, J. Study on the Auxiliary Cementitious Effect of Waste Glass Micro Powder in Recycled Concrete. Master's Thesis, Kunming University of Science and Technology, Kunming, China, 2010.
18. Shi, C.J.; Day, R.L. Comparison of different methods for enhancing reactivity of pozzolans. *Cem. Concr. Res.* **2001**, *31*, 813–818. [CrossRef]
19. Idir, R.; Cyr, M. Pozzolanic properties of fine coarse color-mixed glass cullet. *Cem. Concr. Compos.* **2011**, *33*, 19–29. [CrossRef]
20. Shi, C.; Zheng, K. A review on the use of waste glasses in the production of cement and concrete. *Resour. Conserv. Recycl.* **2007**, *52*, 234–247. [CrossRef]
21. Dyer, T.D.; Dhir, R.K. Chemical Reaction of Glass Cullet used as Cement Component. *Mater. Civ. Eng.* **2001**, *13*, 412–417. [CrossRef]
22. Shi, C.; Wu, Y.; Riefler, C.; Wang, H. Characteristics and pozzolanic reactivity of glass powders. *Cem. Concr. Res.* **2005**, *35*, 987–993. [CrossRef]
23. Archibald, J.F.; DeGagne, D.O.; Lausch, P.; De Souza, E.M. Ground waste glass as a pozzolanic consolidation agent for mine backfill. *CIM Bull.* **1995**, *88*, 80–87.
24. Fan, L.; Liu, G.; Su, H.; Jin, D.; Lu, R.; Li, L. The influence of glass powder particle size distribution on the properties of cementitious materials. *Sci. Technol. Eng.* **2016**, *16*, 271–274.
25. Yue, L.; Ji, T.; Zhou, Y.; Wang, S.; Jiang, M.; Fu, T.; Zhang, S. Active Excitation of Waste Glass Powder and Its Effect on the Properties of Mortar. *Concr. Cem. Prod.* **2022**, *7*, 97–100.
26. Kong, Q. Research on the Activity of Waste Glass Powder by Chemical Excitation and Hydrothermal Excitation. Master's Thesis, South China University, Chiayi, China, 2014.
27. Shi, C.; Day, R.L. Pozzolanic reaction in the presence of chemical activators Part I. Reaction kinetics. *Cem. Concr. Res.* **2000**, *30*, 51–58. [CrossRef]
28. Li, Z. Study on Characterizing the Volcanic ash Activity of Waste Glass Powder Using pH Value and Conductivity. Master's Thesis, South China University, Chiayi, China, 2014.

29. Zhang, C.; Wang, J.; Song, W.; Fu, J. *Effect of Waste Glass Powder on Pore Structure, Mechanical Properties and Microstructure of Cemented Tailings Backfill*; Elsevier Ltd.: Amsterdam, The Netherlands, 2023.
30. Yu, X. Study on The Influence of Glass Powder on The Microcosmic and Mechanical Properties of Concrete. Master's Thesis, Guilin University of Technology, Guilin, China, 2020.
31. Zhao, Y.; Yin, H. *Glass Technology*; Chemical Industry Press: Beijing, China, 2006; Volume 412.
32. Wang, Z.; Zheng, H.; Qian, J. Comparison of sulfate activation on fly ash activity. *Compr. Util. Fly Ash* **1999**, *12*, 15–18.
33. Li, F.; Yang, J.; Li, L. Effect and Mechanism of Waste Glass Powder as Supplementary Cementitious Material on Mortar Properties. *Silic. Bull.* **2022**, *41*, 3208–3218.
34. Lei, F. The Research on Hydration Activity and Mechanism of Cement Paste with Glass Powder. Master's Thesis, Guilin University of Technology, Guilin, China, 2017.
35. Niyomukiza, J.B. Use of waste glass powder in improving the properties of expansive clay soils. *Glob. NEST Int. J. Glob. NEST J.* **2023**, *25*, 139–145.
36. Zhang, W.; Li, S.; Song, L.; Sheng, Y.; Xiao, J.; Zhang, T. Studying the Effects of Varied Dosages and Grinding Times on the Mechanical Properties of Mortar. *Sustainability* **2023**, *15*, 5936. [CrossRef]
37. Xu, Y.; He, T. Effect of Mitigating Strength Retrogradation of Alkali Accelerator by the Synergism of Sodium Sulfate and Waste Glass Powder. *J. Renew. Mater.* **2021**, *9*, 1991–1999. [CrossRef]
38. Dan, J.; Wang, P. Research on the variation law of ion concentration in early cement hydration liquid phase. *J. Shihezi Univ. (Nat. Sci. Ed.)* **2007**, *25*, 494–499.
39. Haha, M.B.; Le Saout, G.; Winnefeld, F.; Lothenbach, B. Influence of activator type on hydration kinetics, hydrate assemblage and microstructural development of alkali activated blast-furnace slags. *Cem. Concr. Res.* **2011**, *41*, 301–310. [CrossRef]
40. Omran, A.F.; Etienne, D.; Harbec, D.; Tagnit-Hamou, A. Long-term performance of glass-powder concrete in large-scale field applications. *Constr. Build. Mater.* **2017**, *135*, 43–58. [CrossRef]
41. Ke, G.; Zou, P.; Gan, Y.; Song, B.; Zeng, D. Strength Activity Characteristic and Mechanism of Waste Glass Powders. *Chin. Powder Technol.* **2015**, *21*, 87–92.
42. Zheng, K.R.; Chen, L.; Zhou, J. Pozzolanic Reaction of Soda-lime Glass and Its influences on Composition of Calcium Silicate Hydrate. *J. Ceram.* **2016**, *44*, 202–210.
43. Tang, Q. Engineering Properties and Mechanism of Soft Soil Solidified by Phosphogypsum—Mineral Powder—Carbide Slag Composite Solid Waste Gelling Agent l. Master's Thesis, Donghua University, Shanghai, China, 2023.
44. Wang, W. Study on the Effect of Stone Powder on the Properties of Alkali-Activated Slag System. Master's Thesis, Guangzhou University, Guangzhou, China, 2023.
45. Li, J. Research on Carbonization of Waste Concrete Powder and Its Application in Brickmaking. Master's Thesis, Guangzhou University, Guangzhou, China, 2023.
46. Liu, G.; Florea, M.V.A.; Brouwers, H.J.H. Waste glass as binder in alkali activated slag–fly ash mortars. *Mater. Struct.* **2019**, *52*, 101. [CrossRef]
47. Bernal, S.A.; Provis, J.; Rose, V.; De Gutierrez, R.M. Evolution of binder structure in sodium silicate-activated slag-metakaolin blends. *Cem. Concr. Compos.* **2011**, *33*, 46–54. [CrossRef]